DOI: 10.1002/ejoc.201000440

Direct Structural Comparison of a Rigid Cyclic Peptidic Scaffold Using Crystallography and NMR in Strained PH Polymer Gels

Christopher J. Arnusch,[a][‡] Johannes H. Ippel,[a][‡] Huub Kooijman,[b] Anthony L. Spek,[b] Rob M. J. Liskamp,[a] Johan Kemmink,*[a] and Roland J. Pieters*[a]

Keywords: NMR spectroscopy / Structure elucidation / Peptides / Amino acids

A small series of biaryl ether containing cyclic peptidic scaffolds was synthesized and cyclized by an S_NAr reaction. The structure of one rigid scaffold was solved by X-ray crystallography and also determined in solution by NMR spectroscopy. Molecular alignment of the peptidic scaffold in strained PH polymer gels in [D_6]DMSO was applied to extract residual dipolar couplings (RDCs). The RDC values were used to obtain a structure that was compared to the crystal structure. Good correlation was obtained, indicating that the RDC method represents a very precise structure determination method for small organic molecules in solution.

Introduction

Residual dipolar couplings are a valuable tool in NMR spectroscopy for structure determination of biological macromolecules.[1] The use of media that induce partial alignment of the molecules reduces the dipolar couplings down to manageable magnitudes of a few Hertz. These so-called residual dipolar couplings (RDCs) are obtained from spectra relatively easily. More recently, the method has been extended for the use of small organic molecules.[2] This too was due to the use of novel media that provide a suitable degree of alignment for the small molecules.[3] The method is most successfully used for rigid compounds, but applications for flexible compounds are also being developed. Useful applications for rigid molecules were found in determining the relative stereochemistry in compounds such as strychnine,[4] menthol,[5] and others.[2b] The method is particularly useful in cases where conventional NMR techniques fail. Besides this, RDCs can in principle also be used for the determination of the 3D structure of small organic molecules and at least they can improve the precision of solution NMR structures. The RDCs determined for cyclosporin A allowed structural refinement of an NOE-determined structure.[6] Furthermore, for the 24-membered macrolide archazolide, RDCs were used in combination with NOEs and *J* couplings to determine the conformation and also the configuration of its 7 stereocenters.[7] In another example, RDCs allowed the distinction to be made between two NMR-derived structures of hormaomycin, a 20-membered ring depsipeptide.[8] Here we describe the detailed molecular structure of a peptidic 14-membered biaryl ether construct (**2**) determined by using RDCs. The determination was performed in DMSO for which strained polymer gels were recently reported.[9] The used gel was a copolymeric crosslinked polyacrylamide gel (PH gel). To gain specific information about the stereochemistry and to have more precise details on the relative orientation of the two rings, "classic" (ROE/NOE and ^3J couplings) NMR constraints are of limited use. Values of distances based on ROE/NOE intensities cannot be measured precisely enough in small molecules to get accurate local angular information on, for example, the two aryl rings. The RDC-derived structure was compared to the structural information obtained by crystal structure analysis and proved to be in excellent agreement, demonstrating the value and utility of the method. Peptidic compound **2** is part of a study involving conformationally restricted biaryl ether containing peptides inspired by natural compounds such as the antibiotic vancomycin[10] and its structural relative complestatin, which has multiple activities including anti-HIV activity.[11] A large spectrum of biological activities is displayed by compounds of the class of cyclic peptides containing biaryl ether linkages.[12] The strained 14-membered cyclophane ring system of cycloisodityrosine[13] is found in several natural products including the antifungal antibiotic piperazinomycin,[14] the series of antitumor antibiotics including bouvardin and RA I–RA XVIII,[12,15] and the metallopeptidase inhibitors K-13[16,17] and OF4949 I-IV[17,18] (see Supporting

[a] Department of Medicinal Chemistry and Chemical Biology, Utrecht Institute for Pharmaceutical Sciences, Utrecht University, P. O. Box 80082, 3508 TB Utrecht, The Netherlands
Fax: +31-30-2536655
E-mail: R.J.Pieters@uu.nl
J. Kemmink@uu.nl
[b] Crystal Structural Chemistry, Utrecht University
Padualaan 8, 3584 CH Utrecht, The Netherlands
[‡] Both authors contributed equally to this work.
Supporting information for this article is available on the WWW under http://dx.doi.org/10.1002/ejoc.201000440.

Information). Furthermore, a related ring structure is present in the antitumor macrocyclic lactones combretastatin DI and D2.[19] An S_NAr cyclization was used to synthesize the biaryl ether linkage.[20]

Results and Discussion

Synthesis

The solution-phase synthesis of the cyclic peptides began with tyrosine, which was protected as a methyl ester on the C-terminus (Scheme 1). Three derivatives were made by coupling this compound to Boc-protected alanine, phenylalanine, and valine with BOP and *i*Pr_2NEt in CH_2Cl_2. Removal of the protecting groups was achieved by TFA/CH_2Cl_2 (1:1) treatment. The N-terminus of the dipeptide was first linked to 1,5-difluoro-2,4-dinitrobenzene by using NEt_3 as a base to give compounds **4**–**6**. These were isolated in overall yields of 65-76% over four steps after column chromatography. 1,5-Difluoro-2,4-dinitrobenzene is highly reactive in nucleophilic aromatic substitutions because of the nitro functionalities in the *ortho* and *para* positions to the carbon atoms bearing a fluorine. Upon substitution with the first nucleophile, the second point of substitution was observed to be slightly less electrophilic, as compounds **4**–**6** were stable yellow solids and could be stored at room temperature for months without degradation. Cyclization was achieved by using K_2CO_3 (4 equiv.) in DMF, which gave highly constrained compounds **1**–**3** in isolated yields of 46–64%. These compounds proved to be very stable in air at room temperature.

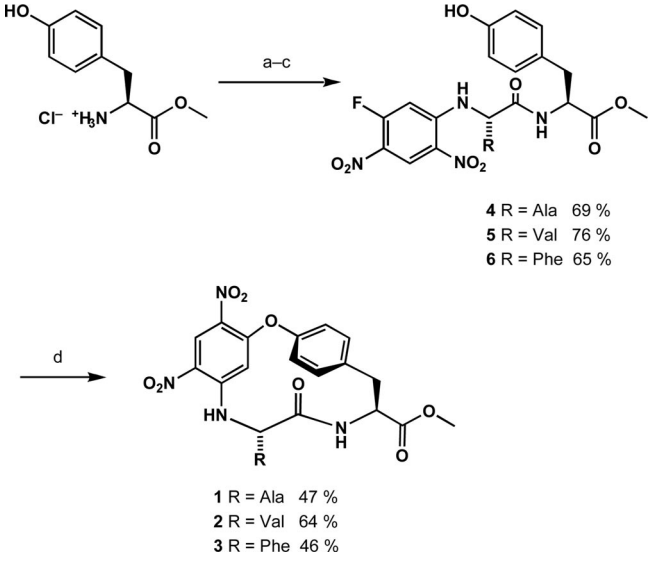

Scheme 1. Synthesis of compounds **1**–**3**. Reagents and conditions: (a) Boc-Xaa-OH, BOP, *i*Pr_2NEt, CH_2Cl_2; (b) TFA/CH_2Cl_2, 1:1; (c) 1,5-difluoro-2,4-dinitrobenzene, NEt_3, 30 min; (d) K_2CO_3, DMF, 3 d, r.t.

Crystal Structure of 2

Crystals for compound **2** were retrieved from a concentrated solution of methanol, and the structure was solved by cryocrystallography at 150 K. The asymmetric unit of the crystal contained two molecules and one methanol solvent molecule (Figure 1). Ring strain in the small cyclic molecule leads to the deformation of the six-membered rings C13–C18 towards a boat conformation. The average absolute endocyclic torsion angle is 4.8 and 5.4° for structures A and B, respectively. The substituent atoms O19 and C12 are located approximately 0.4 Å from the least-squares planes through the six-membered rings. The orientation of the biaryl rings is similar to that found in the crystal structure of piperazinomycin.[14]

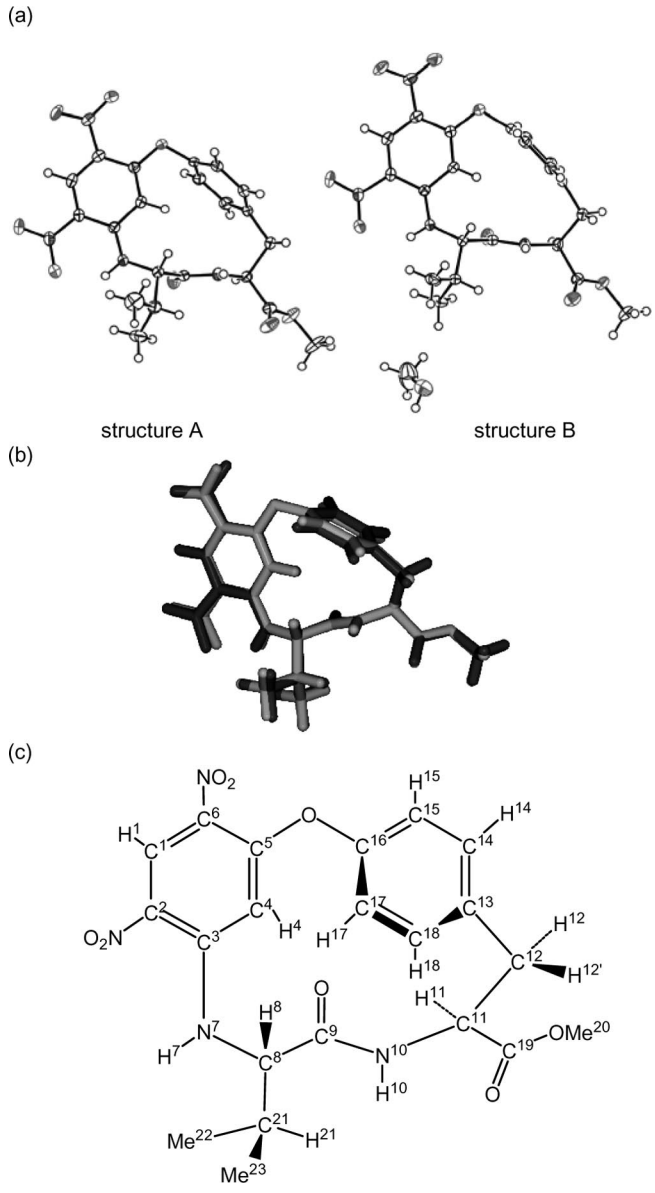

Figure 1. (a) Content of the asymmetric unit of the crystal structure of **2**. Displacement ellipsoids are drawn at the 50% probability level. (b) The two crystallographically independent main molecules have slightly different conformations as shown in a fit-plot. (c) Numbering scheme of **2**.

Solution Structure of 2 Determined by NMR Spectroscopy

Compound **2** was extensively studied by NMR spectroscopy. [D_6]DMSO was chosen as the solvent for reasons of solubility, but also to retain a stable solution when dissolved in strained polymer gels. Complete proton and carbon resonance assignments in the isotropic phase were obtained by a combination of standard ROESY, TOCSY, ^{13}C–^{1}H HSQC, and ^{13}C–^{1}H HMBC 2D spectra. In addition, nitrogen amide resonances could be assigned from a natural abundance ^{15}N–^{1}H HSQC 2D spectrum (see Supporting Information). Analysis of the ROE patterns in the ROESY spectrum of **2** showed that the structure in solution is consistent with that in the crystal. Short distances are observed between H–N10 and H17–H18, but not between H–N10 and H14–H15 (see Figure 1c for the numbering scheme). These distances are consistent with a rigid orientation of the ring C13–C18, in which H17 and H18 are positioned over the amide backbone at position N10, whereas on the back of the molecule H11 is placed close to H14, but not H18. Moreover, two ROEs with equal intensity are found between either H4 and H15 or H4 and H17, which indicates that the two aryl rings are more or less placed perpendicular to each other. This perpendicular orientation also explains the unusual shifted resonance of the aromatic H4 proton signal at 4.109 ppm. The H4 proton is considerably shifted upfield, because of its position in the strongly shielded ring current field of the opposite aryl ring C13–C18. Stereospecific assignment of the methylene H12 and H12′ protons follows from the large vicinal coupling constant of 12.3 Hz observed between H11 and H12′ (and between H11–H12, J = 5.3 Hz) and the large ROE between H11 and H12 (with ROE H11–H12′ absent). Such a combination is only possible with a *trans* configuration between protons H11 and H12′.

NMR in Strained PH Gels

Even though the NMR structure is consistent with the crystal structure, it cannot provide the same level of structural detail. The RDCs have the potential to greatly improve the level of detail. Partial alignment of **2** in strained polymer gels was used to extract the RDCs. The alignment was achieved by use of the copolymeric cross-linked polyacrylamide (PH) gel as the preferred alignment medium that is compatible with DMSO.[9] The amount of alignment can be tuned by reswelling the dried polymerized gel in smaller diameter tubes and/or by increasing the percentage of monomer concentration in the copolymerization step. In this study, 8 and 12% PH gels were made inside 5 mm NMR tubes and equilibrated for 7 and 14 d, respectively, with a solution of **2** in [D_6]DMSO. The diffusion process into the clear transparent gel was easily monitored because of the dark yellow colored solution of **2**. After sufficient time, duplicate measurements of **2** in the 8% PH gel showed that a stable solution was maintained in the gel over time. The degree of alignment in the media can be measured from the quadrupolar splitting of the solvent line in the deuterium NMR spectrum and amounts to 2.5 Hz and less than 1.6 Hz (within the natural line width) for the 12 and 8% gel sample, respectively. To measure the RDCs, t_2-coupled ^{13}C–^{1}H HSQC spectra and t_2-coupled ^{15}N–^{1}H HSQC spectra were recorded in the presence (anisotropic solution) and absence (isotropic solution) of the orienting gel. The scalar $^{1}J_{CH}$ and $^{1}J_{NH}$ and total couplings $^{1}J_{CH}$ + $^{1}D_{CH}$ (and $^{1}J_{NH}$ + $^{1}D_{NH}$) were measured individually after extraction of 1D F2 traces from the HSQC spectra. The difference between the two coupling constants then results in the RDCs $^{1}D_{CH}$ (or $^{1}D_{NH}$). An overlay of the t_2-coupled ^{13}C–^{1}H HSQC spectrum of **2** in the isotropic solution and the anisotropic solution (8% PH gel) is shown in Figure S4 (Supporting Information). The carbon-bound proton signals of the PH gel matrix show up as residual broad doublet signals in the spectrum in the 8% PH gel solution. Interference of the broad polymer signals (NMe and CH_2 from DMAA, and NH and CH_2 from AMPS; for the structures, see Figure S3, Supporting Information) is also visualized by the corresponding 1D proton spectrum inside the 2D HSQC spectrum. The large polymer signals appear rather high in the 1D spectrum but are strongly reduced in intensity due to efficient spin relaxation when measured by 2D correlation spectra. Figure 2 shows slices through the H18 carbon resonance of the t_2-coupled ^{13}C–^{1}H HSQC spectra of the isotropic and two anisotropic solutions, with their respective RDC values obtained after curve-fitting the line shape of the ^{13}C-coupled proton resonance signals. As shown in Figure 2, increased alignment was associated with higher anisotropy; hence, larger line widths were present along the proton dimension. Table 1 summarizes the final determined

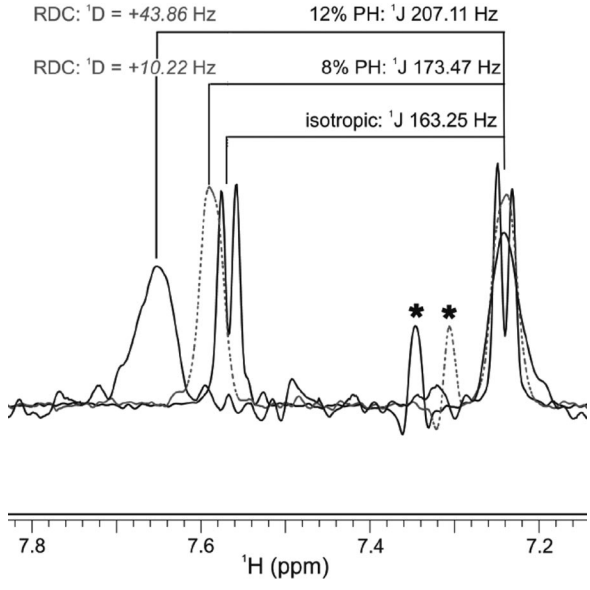

Figure 2. Cross-section taken at the ω_1 frequency of carbon C18 of the isotropic t_2-coupled ^{1}H-^{13}C HSQC spectrum aligned with cross-sections of the spectra recorded in the 8 and 12% PH gels. The observed $^{1}J_{HC}$ + $^{1}D_{HC}$ coupling constants of each spectrum are indicated together with the dipolar $^{1}D_{HC}$ coupling constants in the 8 and 12% PH gel, respectively. Peaks indicated with an asterisk originate from the H14–C14 correlation.

RDC values of all protons in **2**. In both alignment media, relative weak alignment was observed with values of $^1D_{CH}$ (or $^1D_{NH}$) that are always substantially smaller than $^1J_{CH}$ (or $^1J_{NH}$).

Table 1. Isotropic one-bond ^{15}N–^1H coupling constants $^1J_{NH}$ and ^{13}C–^1H coupling constants $^1J_{CH}$ (Hz) of **2** in [D_6]DMSO, together with corresponding RDC (defined as $^1Dij - {}^1J_{CH}$) (Hz) determined in duplo from two different aligned PH media, all recorded at 27 °C.

Proton pair	$^1J_{NH}/^1J_{CH}$ [Hz]	RDC (8%PH gel) [Hz]	RDC (12%PH gel) [Hz]
H–N7	94.01	–1.95	–10.21
H–N10	92.01	3.61	(+29)[a,b]
H1–C1	169.72	–1.17	–10.34
H4–C4	163.48	–1.32	–11.30
H14–C14	161.11	1.31	13.23
H15–C15	164.47	9.66	38.57
H17–C17	164.89	1.38	13.92
H18–C18	163.25	9.53	43.86
H8–C8	140.91	2.42	11.84
H11–C11	141.49	10.01	43.58
H12–C12	132.93	–1.65	–4.27
H12′–C12	131.42	(+14)[a]	(N.D.)[a,c]
H21–C21	130.88	1.92	1.31
Me20–C20	147.74	0.75[d]	5.00[d]
Me22–C22	126.04	–0.16[d]	–1.08[d]
Me23–C23	126.17	0.06[d]	–0.09[d]

[a] Partial overlap with signals of the polymer PH matrix. The absolute size and sign of the RDC is in agreement with predicted values, but was not used in the RDC fitting procedure. [b] No accurate value of RDC due to low signal-to-noise ratio. Estimated error limit is 29 ± 10 Hz. [c] Not determined, too broad signal overlapping with resonances of the polymer PH matrix. [d] Time-averaged RDC values of methyl protons, not used in the RDC fitting procedure.

PALES Alignment Fit Procedure

The single-value decomposition module (SVD)[21] of the program PALES[22] was used to fit 12 (in case of the 8% gel) or 11 (in case of the 12% gel) experimental dipolar couplings to the reference crystal structures A and B (Figure 1). Due to partial overlap of H12′ with residual signals of the polymer matrix, the RDC of H12′ was not included in the fit. The predicted RDC values do show the correct sign and amplitude as estimated from the experiment. Moreover, the imprecise value of $^1D_{NH}$ (H-N10), obtained from the spectrum in the 12% PH gel solution, was excluded from the fit.

Typical fits of the experimental RDCs, derived from both the 8 and 12% PH gel NMR spectroscopic data versus predicted RDCs calculated from different types of reference structures are displayed in Figure 3. Correlation factors and statistics for these fits are given in the Supporting Information. In the first panel (Figure 3a), the 8% PH gel correlation plot is shown with respect to the original atomic coordinates of the reference crystal structures: structure B. The correlation factor R is 0.970 with a root mean squares deviation (RMSD) of the experimental RDC data points just above 1.02 Hz. At this point, it is good to know that the PALES fit relies on correct covalent atomic bond lengths to calculate the alignment tensor and scale the relative size of

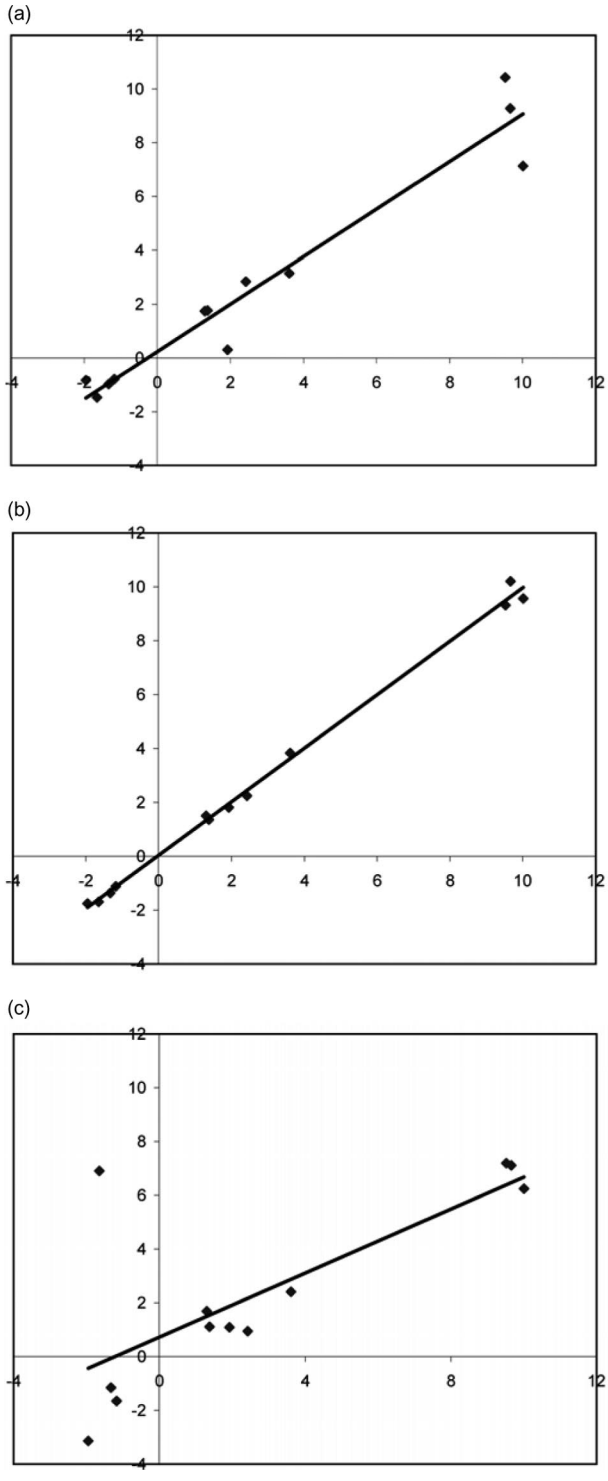

Figure 3. Correlation plots between the calculated (vertical axis) and the observed RDCs in case of the 8% PH gel (horizontal axis). (a) The calculated RDCs derived from X-ray structure B (R = 0.970) and (b) from the SA energy-minimized computer model (R = 0.998); (c) same as (b) but with an intentional erroneous switch between the assignments of H12 and H12′ to illustrate the sensitivity of the method (R = 0.739).

the dipolar couplings. Normally, the electron density at the center of the hydrogen atoms in crystallography is too low to accurately determine hydrogen bond lengths. Not surprisingly, a significant improvement in the PALES fit (R = 0.992 and RMSD = 0.575 Hz) is obtained after energy-minimization (Amber99 force field) of the hydrogen atom positions (with all heavy atoms fixed). Comparison to structure A yielded almost the same fits. In the next step, the newly hydrogen-built reference crystal structures of **2** were subjected to a low temperature (300 K) simulated annealing (SA) step in a pre-equilibrated box of DMSO molecules, again by applying a sophisticated force field calculation. Improvements in the fits are observed, but mainly for the structure starting from structure B of the crystal structure. In this case, the correlation factor increased to 0.998, whereas at the same time the RMSD decreased to 0.24 Hz, leading to a perfect fit that falls well within the experimental error limits (Figure 3b).

A similarly good correlation (R = 0.997 and RMSD = 1.67 Hz) was obtained between the RDC values that are independently determined from the 12% PH gel data and the RDC values calculated from the computer energy-minimized structure B. The energy-minimized crystal structure A led to a slightly less optimal fit. To illustrate how critical the PALES SVD procedure works to get a unique solution for **2** based on experimental RDC values alone is demonstrated in Figure 3c. This plot shows that the good correlation between experimental and predicted RDCs drops dramatically when RDCs are not correctly assigned, such as in the case of the reversal of H12 and H12′ assignments and the 8% PH gel data.

Conclusions

The conclusion is that one particular energy-minimized conformer derived from one of the two crystal structures (structure B) agrees best with the experimentally determined RDC data in solution. Figure 1b shows an overlay of the two crystal substructures, which reveals a small difference in the relative orientation of the biaryl rings and the two NO_2 groups (RMSD heavy atom 0.26 Å). The comparison between the structure that best fits the RDC values, that is, the energy minimized computer model derived from structure B, and structure B itself is shown in Figure 4. Here, the structural differences are even less (RMSD heavy atom 0.22 Å). The RDC-based structure determination for rigid compound **2** is remarkably precise, as it is possible to distinguish between very similar structures of **2**. Small imperfections in the match between calculated and observed RDCs readily show up as a lower correlation, that is, a lower R value. Therefore, RDC-based structure determination is a good alternative to X-ray crystallography for conformationally homogeneous cyclic peptides.

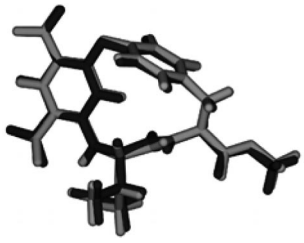

Figure 4. Overlap of the X-ray structure of **2** (structure B, black) with the optimal RDC-derived structure (gray).

Experimental Section

General Remarks: Chemicals were obtained from commercial sources and used without further purification unless stated otherwise. DMF, CH_2Cl_2, and CH_3OH were purchased from Biosolve, the Netherlands. CH_2Cl_2 and DMF were stored over 4 Å molecular sieves, and CH_3OH was stored over 3 Å molecular sieves. iPr$_2$NEt was obtained from Acros Organics, and HPLC-grade TFA was obtained from Merck. The bases iPr$_2$NEt and Et$_3$N were distilled from ninhydrin and KOH. The coupling reagent benzotriazol-1-yloxy-tris(dimethylamino)phosphonium hexafluorophosphate (BOP)[23] was obtained from Richelieu Biotechnologies Inc. (Montreal, Canada). Column chromatography was performed on ICN Silica 32-63, 60 Å. Thin-layer chromatography (TLC) was performed on Merck precoated Silica 60 plates. Visualization was accomplished with UV light and staining with ninhydrin. Amino acids were purchased from Multisyntech. Electrospray ionization (ESI) mass spectrometry was carried out using electrospray MS (nano ESI-TOF-MS) run with a Micromass LC–TOF mass spectrometer by spraying a 90% MeOH solution of **1** from a gold-coated glass capillary in a Z-spray nanospray ionization source or by using a Shimadzu LCMS QP-8000 single quadrupole bench top mass spectrometer (m/z range < 2000), coupled with a QP-8000 data system.

General NMR Spectroscopy: ^{1}H NMR spectra were recorded with a Varian G-300 spectrometer (300 MHz) or a Varian INOVA spectrometer (500 MHz). ^{13}C NMR spectra were recorded with a Varian G-300 spectrometer at 75.4 MHz. All spectra were referenced to the solvent signal of CD_3OD(H) [δ(^{1}H) = 3.3 ppm, δ(^{13}C) = 49.0 ppm] or [D$_6$]DMSO [δ(^{1}H) = 2.49–2.50 ppm, δ(^{13}C) = 39.5 ppm]. Complete assignment of proton, carbon, and amide nitrogen atoms for **1** in [D$_6$]DMSO were made by using a combination of 2D TOCSY (mixing times 20 and 60 ms), 2D ROESY (mixing times 150, 300, and 500 ms), 2D ^{1}H–^{13}C HSQC, 2D ^{1}H–^{13}C HMBC (60 ms filter delay), and 2D ^{1}H–^{15}N HSQC spectra. Scalar coupling constants were measured from a high-resolution 1D NMR spectrum. All spectra were processed and analyzed with MestRe-C.

Strained Gel NMR Spectroscopy: After recording the reference NMR spectra of **2** in the isotropic phase, two different strained PH gel samples were prepared. The PH gel was made by copolymerization of 2-(acryloamido)-2-methylpropanesulfonic acid (AMPS) monomer with N,N-dimethylacrylamide (DMAA) as comonomer in the presence of N,N'-methylenebisacrylamide (BIS) as crosslinker and ammonium persulfate (APS) as radical initiator[24,9] (see also Supporting Information for structural formulas). The procedure for making the PH gel and letting the dried gel reswell in [D$_6$]DMSO inside a 5 mm NMR tube is described in the literature.[9] In this case, the isolated PH gel samples were first measured to check that no residual NMR peaks from unreacted monomers are present in the PH polymer gel after the washing steps. Two different strengths of strained gel samples were used: 8% (w/v) and 12% (w/v) made by addition of a concentrated stock solution of **2**

in [D_6]DMSO on top of the preswollen gel. Diffusion of the yellowish colored compound into the gel was achieved in 7 and 14 d for the 8 and 12% gel sample, respectively, a process that could be optically followed in time to ensure a homogeneous solution for that part of the sample that is positioned at the height of the NMR receiver coil.

Proton t_2-^{13}C-coupled HSQC spectra were acquired at natural abundance as 2048 × 512 data point matrices (2048 × 86 matrix for t_2-^{15}N-coupled HSQC spectra), processed by sine bell square multiplication and zero-filled in both dimensions to a final digital resolution of 0.73 Hz/pt in the proton acquisition dimension, and to a resolution of 12.2 and 3.9 Hz/pt in the heteronuclear ^{13}C and ^{15}N dimension, respectively. Extraction of scalar ($^1J_{C/N-H}$) and/or the sum of scalar and residual dipolar couplings ($^1J_{C/N-H}$ + $^1D_{C/N-H}$) were done by taking 1D slices of proton cross peaks at the carbon or nitrogen frequency of interest and compare them. Precise values of the RDC were determined by curve-fitting the relative position of proton resonance lines from the multiplet patterns in both the isotropic reference and the PH gel spectra. Error limits are estimated (based on an independent duplo measurement of the 8% PH gel sample and based on different ways of processing the NMR spectroscopic data) to ±0.2 Hz for RDCs, belonging to intense aromatic and methyl protons, and to ±0.3 Hz for RDCs of other signals, unless stated otherwise.

Pales Calculations: The single-value decomposition module (SVD)[21] of the program PALES[22] was used to analyze the experimental determined RDC values. Tensor alignment was done by simultaneous fitting of the Saupe alignment matrix and the degree of alignment (Da, Dr), a situation well applicable due to the high number (11 to 12) of available experimental RDC restraints with respect to the degrees of fit variables. The four Pales parameters: correlation factor *r*, RMSD, Bax slope, and Chi square, were evaluated together in the judgment of best fit.

Amber99 Energy-Minimization Calculations: Crystal structures of **2** in mmCIF format were converted to PDB format using Yasara Structure (www.yasara.org), with both the residue- and atom naming convention largely restructured to L-amino acid topology. An accurate description of the molecular geometry for **2** has been obtained by applying the Amber99 force field in Yasara energy calculations, making use of self-parametrized force field parameters and quantum-mechanically derived AM1 derived atomic charges. Energy-minimization (simulated annealing from 300 K to zero Kelvin) of the two crystal molecules in the unit cell were carried in two ways: (i) optimization of protons with all heavy atoms fixed in vacuo; (ii) optimization of all atoms in explicit DMSO solvent. In the latter case, the fixed solute was placed into a pre-equilibrated periodic box of DMSO solvent molecules (density 1.10 g/mL) and equilibrated for another 500 ps of molecular dynamics under periodic boundary conditions (time step 1 fs, nonbonded cutoff 7.86 Å, Ewald summation of long-range electrostatics, constant pressure at a density of 1.10 g/mL) before slowly free up the solute and running a full simulated annealing energy minimization on the total system. Distance and angle measurements, as well as RMSD fits were also carried out in Yasara Structure.

X-ray Crystallography: CCDC-769665 (for **2**) contains the supplementary crystallographic data for this paper. These data can be obtained free of charge from The Cambridge Crystallographic Data Centre via www.ccdc.cam.ac.uk/data_request/cif.

Synthesis of 4–6: H-Tyr(OH)-OMe (200 mg, 1.03 mmol), Boc-Xaa-OH (Boc-Ala-OH 195 mg, 1.03 mmol; Boc-Val-OH 224 mg, 1.03 mmol; Boc-Phe-OH 273 mg, 1.03 mmol), and BOP (455 mg, 1.03 mmol) were measured into a 100-mL round-bottomed flask equipped with a stir bar. CH_2Cl_2 (15 mL) and *i*Pr_2NEt (0.538 mL, 3.1 mmol) were added, and the solution was stirred at room temperature for 3 h. CH_2Cl_2 was removed in vacuo, and EtOAc was added (50 mL). The organic solution was washed with 1 N $KHSO_4$, 5% $NaHCO_3$, and brine (each 2 × 50 mL) and then dried with Na_2SO_4. The resulting products were tested with TLC [R_f = 0.21 (Ala, Val), R_f = 0.24 (Phe); CH_2Cl_2/MeOH, 19:1] and were used without further purification. Each product was dissolved in CH_2Cl_2 (10 mL) and to it was added TFA (10 mL) at 0 °C. The solutions were stirred for 4 h at room temperature. After evaporation and multiple coevaporation with EtOH and CH_2Cl_2 in vacuo, the crude products were dissolved in EtOAc (20 mL). To each was added Et_3N (0.43 mL, 3.1 mmol) and a solution of 1,5-difluoro-2,4-dinitrobenzene (210 mg, 1.03 mmol) in EtOAc (20 mL). The pH was tested and observed as basic. After 45 min the solvents were removed in vacuo and **4**–**6** were purified by column chromatography (EtOAc/hexane, 1.5:1). Data for **4**: 321 mg (69%). R_f = 0.67 (EtOAc). ^{1}H NMR (CD_3OD): δ = 1.49 (d, *J* = 7 Hz, 3 H), 2.89 (dd, *J* = 9, 14 Hz, 1 H), 3.11 (dd, *J* = 6, 14 Hz, 1 H), 3.69 (s, 3 H) 4.27 (q, *J* = 7 Hz, 1 H), 4.66 (q, *J* = 5 Hz, 1 H), 6.62 (m, 2 H, 1 H), 6.97 (d, *J* = 8 Hz, 2 H), 9.04 (d, *J* = 8 Hz, 1 H) ppm. MS: *m*/*z* = 431 [M + H]$^+$. Data for **5**: 375 mg (76%). R_f = 0.72 (EtOAc). ^{1}H NMR (CD_3OD): δ = 0.98 (d, *J* = 6 Hz, 6 H), 2.19 (m, 1 H), 2.84 (dd, *J* = 10, 14 Hz, 1 H), 3.14 (dd, *J* = 5, 14 Hz, 1 H), 3.69 (s, 3 H), 3.97 (d, *J* = 5 Hz, 1 H), 4.75 (m, 1 H), 6.56 (d, *J* = 9 Hz, 2 H), 6.65 (d, *J* = 14 Hz, 1 H), 6.94 (d, *J* = 9 Hz, 2 H), 9.05 (d, *J* = 8 Hz, 1 H) ppm. Data for **6**: 350 mg (65%). R_f = 0.77 (EtOAc). ^{1}H NMR (CD_3OD): δ = 2.86 (dd, *J* = 9, 14 Hz, 1 H), 3.03-3.11 (m, 2 H), 3.23 (dd, *J* = 5, 14 Hz, 1 H), 3.69 (s, 3 H), 4.46 (dd, *J* = 5, 8 Hz, 1 H), 4.70 (dd, *J* = 5, 9 Hz, 1 H), 6.47 (d, *J* = 14 Hz, 1 H), 6.59 (d, *J* = 8 Hz, 2 H), 6.94 (d, *J* = 8 Hz, 2 H), 7.20-7.27 (m, 5 H), 8.97 (d, *J* = 8 Hz, 1 H) ppm.

Synthesis of 1: To a round-bottomed flask equipped with a stir bar was added **4** (39 mg, 0.09 mmol) in DMF (50 mL). K_2CO_3 (43 mg, 0.31 mmol) was added, and the yellow solution became dark red. This solution was stirred protected from light for 5 d. AcOH was added (≈1 mL), and the color changed from a dark red to a light orange. The solvents were removed in vacuo. Product **1** was purified by column chromatography (EtOAc/toluene, 1:1) to yield 17.4 mg (47%) of a yellow solid. R_f = 0.47 (EtOAc). ^{1}H NMR ($CDCl_3$): δ = 1.57 (d, *J* = 8 Hz, 3 H), 2.70 (t, *J* = 13 Hz, 1 H), 3.47 (dd, *J* = 6 Hz, 1 H), 3.70 (dd, *J* = 6, 13.5 Hz, 1 H)), 3.84 (s, 3 H) 4.14 (s, 1 H), 4.98 (m, 1 H), 5.63 (d, *J* = 10.5 Hz, 1 H), 6.99 (dd, *J* = 2, 9 Hz, 1 H), 7.24 (m, 2 H), 7.49 (dd, *J* = 2, 9 Hz, 1 H), 7.93 (d, *J* = 3.5 Hz, 1 H), 9.04 (s, 1 H) ppm. ^{13}C NMR ([D_6]DMSO): δ = 18.9, 36.4, 52.2, 52.6, 54.9, 102.0, 122.9, 123.3, 125.1, 126.6, 127.5, 132.0, 132.9, 137.3, 147.0, 154.2, 160.9, 169.4, 171.4 ppm. MS: *m*/*z* = 431 [M + H]$^+$.

Synthesis of 2: To a round-bottomed flask equipped with a stir bar was added **5** (259 mg, 0.54 mmol) in DMF (275 mL). K_2CO_3 (300 mg, 2.17 mmol) was added, and the yellow solution became dark red. This solution was stirred protected from light for 5 d. AcOH was added (≈10 mL), and the color changed from a dark red to a light orange. EtOAc (500 mL) and H_2O (250 mL) were added, and the two phases were separated. The EtOAc layer was washed with H_2O (3 × 400 mL) and brine, and dried with Na_2SO_4. The solvent was removed in vacuo, and the residue was purified by column chromatography (EtOAc/toluene, 1:1) to yield 158 mg (64%) of a yellow solid. R_f = 0.53 (EtOAc). ^{1}H NMR (CD_3OD): δ = 0.99 (d, *J* = 7 Hz, 3 H), 1.09 (d, *J* = 7 Hz, 3 H), 2.27 (m, 1 H), 2.82 (t, *J* = 13 Hz, 1 H), 3.44 (d, *J* = 4 Hz, 1 H), 3.66 (dd, *J* = 8, 13 Hz, 1 H), 3.79 (s, 3 H), 4.19 (s, 1 H), 4.88 (m, 1 H), 6.93 (dd, *J* = 2, 9 Hz, 1 H), 7.30 (dd, *J* = 2, 9 Hz, 1 H), 7.37 (dd, *J* = 2, 9 Hz,

1 H), 7.50 (dd, J = 2, 9 Hz, 1 H), 8.92 (s, 1 H) ppm. ^{13}C NMR ([D$_6$]DMSO): δ = 16.8, 19.4, 30.8, 36.2, 52.2, 52.6, 61.7, 101.8, 123.0, 123.2, 125.2, 126.7, 127.6, 132.0, 132.8, 137.3, 147.6, 154.3, 161.0, 167.9, 171.3 ppm. MS: m/z = 459 [M + H]$^+$.

Synthesis of 3: To a round-bottomed flask equipped with a stir bar was added **6** (54 mg, 0.10 mmol) in DMF (50 mL). K_2CO_3 (43 mg, 0.31 mmol) was added, and the yellow solution became dark red. This solution was stirred protected from light for 5 d. AcOH was added (≈1 mL), and the color changed from a dark red to a light orange. The solvents were removed in vacuo. Compound **3** was purified by column chromatography (EtOAc/toluene, 1:1) to yield 24 mg (46%) of a yellow solid. R_f = 0.60 (EtOAc). ^{1}H NMR (CD_3OD): δ = 2.86 (t, J = 13 Hz, 1 H), 3.03 (dd, J = 9, 13 Hz, 1 H), 3.24 (dd, J = 4, 14 Hz, 1 H), 3.69 (dd, J = 4, 14 Hz, 1 H), 3.78 (dd, J = 4, 9 Hz, 1 H), 3.84 (s, 3 H), 4.19 (s, 1 H), 4.91 (m, 1 H), 6.93 (dd, J = 2, 9 Hz, 1 H), 7.24 (m, 1 H), 7.31 (m, 5 H), 7.41 (dd, J = 2, 9 Hz, 1 H), 7.52 (dd, J = 2, 9 Hz, 1 H), 8.87 (s, 1 H) ppm. ^{13}C NMR ([D$_6$]DMSO): δ = 36.5, 37.6, 52.3, 52.7, 58.1, 102.0, 123.1, 123.3, 124.9, 126.7, 127.1, 127.6, 128.6, 129.1, 132.1, 132.7, 135.9, 137.3, 146.9, 154.2, 160.9, 167.9, 171.4 ppm. MS: m/z = 507 [M + H]$^+$.

Supporting Information (see footnote on the first page of this article): X-ray structures of current compound and related natural products, chemical shift and coupling constants of **2**, components of the PH gel, and correlation factors between calculated and observed RDCs.

[1] a) N. Tjandra, A. Bax, *Science* **1997**, *278*, 1111–1114; b) J. H. Prestgard, A. I. Kishore, *Curr. Opin. Chem. Biol.* **2001**, *5*, 584–590.
[2] a) R. M. Gschwind, *Angew. Chem. Int. Ed.* **2005**, *44*, 4666–4668; b) C. M. Thiele, *Eur. J. Org. Chem.* **2008**, 5673–5685.
[3] C. M. Thiele, *Concepts Magn. Reson. A* **2004**, *30A*, 65–80.
[4] C. M. Thiele, *J. Org. Chem.* **2004**, *69*, 7403–7413.
[5] L. Verdier, P. Sakhaii, M. Zweckstetter, C. Griesinger, *J. Magn. Reson.* **2003**, *163*, 353–359.
[6] J. Klages, C. Neubauer, M. Coles, H. Kessler, B. Luy, *ChemBioChem* **2005**, *6*, 1672–1678.
[7] C. Farès, J. Hassfeld, D. Menche, T. Carlomagno, *Angew. Chem. Int. Ed.* **2008**, *47*, 3722–3726.
[8] U. Reinscheid, J. Farjon, M. Radzom, P. Haberz, A. Zeeck, M. Blackledge, C. Griesinger, *ChemBioChem* **2006**, *7*, 287–296.
[9] P. Haberz, J. Farjon, C. Griesinger, *Angew. Chem. Int. Ed.* **2005**, *44*, 427–429.
[10] G. H. Singh, H. Jayasuriya, D. L. Hazudda, P. Felock, C. F. Homnick, M. Sardana, A. Patane, *Tetrahedron Lett.* **1998**, *39*, 8769–8770.
[11] J. Garfunkle, F. S. Kimball, J. D. Trzupek, S. Takizawa, H. Shimamura, M. Tomishima, D. L. Boger, *J. Am. Chem. Soc.* **2009**, *131*, 16036–16038.
[12] L. Feliu, M. Planas, *Int. J. Pept. Res. Ther.* **2005**, 53–97.
[13] a) A. Bigot, J. Zhu, *Tetrahedron Lett.* **1998**, *38*, 551–554; b) P. J. Krenitsky, D. L. Boger, *Tetrahedron Lett.* **2002**, *43*, 407–410; c) O. Poupaardin, F. Ferreira, J. P. Genet, C. Greck, *Tetrahedron Lett.* **2001**, *42*, 1523–1526; d) A. Bigot, M. E. T. H. Dau, J. Zhu, *J. Org. Chem.* **1999**, *64*, 6283–6296.
[14] a) S. Tamai, M. Kaneda, S. Nakamura, *J. Antibiot.* **1982**, *35*, 1130–1136; b) S. Nishiyama, K. Nakamura, Y. Suzuki, S. Yamamura, *Tetrahedron Lett.* **1986**, *37*, 4481–4484; c) S. Ghosh, A. S. Kumar, G. N. Mehta, R. Sounderarajan, S. Sen, *Arkivoc* **2009**, *7*, 72–78.
[15] a) S. D. Jolad, J. J. Hoffmann, S. J. Torrance, R. M. Wiedhopf, J. R. Cole, S. K. Arora, R. B. Bates, R. L. Gargiulo, G. R. Kriek, *J. Am. Chem. Soc.* **1977**, *99*, 8040; b) J.-E. Lee, Y. Hitotsuyanagi, I.-H. Kim, T. Hasuda, K. Takeya, *Bioorg. Med. Chem. Lett.* **2008**, *18*, 808–811.
[16] H. Kase, M. Kaneko, K. Yamado, *J. Antibiot.* **1987**, *40*, 450–454.
[17] J. W. Janetka, D. H. Rich, *J. Am. Chem. Soc.* **1997**, *119*, 6488–6495.
[18] a) S. Sano, K. Ikai, H. Kuroda, T. Nakamura, A. Obayashi, Y. Ezure, H. Enomoto, *J. Antibiot.* **1986**, *39*, 1674–1684; b) S. Sano, K. Ikai, K. Katayama, K. Takesako, T. Nakamura, A. Obayashi, Y. Ezure, H. Enomoto, *J. Antibiot.* **1986**, *39*, 1685–1696; c) S. Sano, M. Ueno, K. Katayama, T. Nakamura, A. Obayashi, *J. Antibiot.* **1986**, *39*, 1697–1703; d) S. Sano, K. Ikai, Y. Yoshikawa, T. Nakamura, A. Obayashi, *J. Antibiot.* **1987**, *40*, 512–518; e) S. Sano, H. Kuroda, M. Ueno, Y. Yoshikawa, T. Nakamura, A. Obayashi, *J. Antibiot.* **1987**, *40*, 519–525.
[19] G. R. Pettit, P. D. Quistorf, J. A. Fry, D. L. Herald, E. Hamel, J.-C. Chapuis, *J. Nat. Prod.* **2009**, *72*, 876–883.
[20] a) C. J. Arnusch, R. J. Pieters, *Tetrahedron Lett.* **2004**, *45*, 4153–4156; b) C. J. Arnusch, R. J. Pieters, *Eur. J. Org. Chem.* **2003**, 3131–3138.
[21] J. A. Losonczi, M. Andrec, M. W. F. Fischer, J. H. Prestegard, *J. Magn. Reson.* **1999**, *138*, 334–342.
[22] M. Zweckstetter, A. Bax, *J. Am. Chem. Soc.* **2000**, *122*, 3791–3792.
[23] B. Castro, J. R. Dormoy, G. Evin, C. Selve, *Tetrahedron Lett.* **1975**, *16*, 1219–1222.
[24] X. Liu, Z. Tong, F. Gao, *Polym. Int.* **1998**, *31*, 215–220.

Received: April 1, 2010
Published Online: July 7, 2010

